Chaoyong He,[1] Hongliang Li,[1] Benoit Viollet,[2,3,4] Ming-Hui Zou,[1] and Zhonglin Xie[1]

CrossMark

AMPK Suppresses Vascular Inflammation In Vivo by Inhibiting Signal Transducer and Activator of Transcription-1

COMPLICATIONS

Activation of AMPK suppresses inflammation, but the underlying mechanisms remain poorly understood. This study was designed to characterize the molecular mechanisms by which AMPK suppresses vascular inflammation. In cultured human aortic smooth muscle cells, pharmacologic or genetic activation of AMPK inhibited the signal transducer and activator of transcription-1 (STAT1), while inhibition of AMPK had opposite effects. Deletion of AMPKα1 or AMPKα2 resulted in activation of STAT1 and in increases in proinflammatory mediators, both of which were attenuated by administration of STAT1 small interfering RNA or fludarabine, a selective STAT1 inhibitor. Moreover, AMPK activation attenuated the proinflammatory actions induced by STAT1 activators such as interferon-γ and angiotensin II (AngII). Mechanistically, we found that AMPK activation increased, whereas AMPK inhibition decreased, the levels of mitogen-activated protein kinase phosphatase-1 (MKP-1), an inducible nuclear phosphatase, by regulating proteasome-dependent degradation of MKP-1. Gene silencing of MKP-1 increased STAT1 phosphorylation and prevented 5-amino-imidazole-4-carboxyamide ribonucleoside–reduced STAT1 phosphorylation. Finally, we found that infusion of AngII caused a more severe inflammatory response in AMPKα2 knockout mouse aortas, all of which were suppressed by chronic administration of fludarabine. We conclude that AMPK activation suppresses STAT1 signaling and inhibits vascular inflammation through the upregulation of MKP-1.

Chronic low-grade inflammation is an important pathogenic factor in the development of type 2 diabetes and cardiovascular diseases (1). The metabolic abnormalities of type 2 diabetes, including hyperglycemia, dyslipidemia, and insulin resistance, activate the Janus kinases/signal transducer and activator of transcription (JAK/STAT) signaling pathway, a major intracellular inflammatory cascade that transmits the intracellular signaling to the nucleus (2), promoting inflammatory response, inducing insulin resistance (3), and accelerating the development of cardiovascular complications (4). In the vasculature, activation of STAT1 and STAT3 promotes inflammatory response (5), increases neointimal formation (6), and accelerates the development of atherosclerosis (7), a chronic disease characterized by inflammation in the artery wall (8). Conversely, inhibition of STAT3 improves insulin sensitivity (3). Deletion of STAT1 attenuates the progression of atherosclerosis (9). Thus, the JAK/STAT pathway is an attractive therapeutic target for treating metabolic and cardiovascular diseases.

AMPK is a trimeric enzyme that contains a catalytic α-subunit and regulatory β- and γ-subunits (10). In addition to regulating energy metabolism, AMPK participates in the regulation of many other cellular processes, including autophagy, apoptosis (11–14), and inflammation. For example, reduction of AMPK activity is associated with inflammation in metabolic syndrome, including obesity and type 2 diabetes (1,15). In addition, AMPK activation promotes macrophage polarization to an anti-inflammatory phenotype (16), prevents the nuclear translocation of nuclear factor-κB (NF-κB), and inhibits the proinflammatory actions of interferon-γ (IFN-γ) and tumor necrosis

[1]Section of Molecular Medicine, Department of Medicine, University of Oklahoma Health Sciences Center, Oklahoma City, OK
[2]INSERM U1016, Institut Cochin, Paris, France
[3]CNRS UMR 8104, Paris, France
[4]Université Paris Descartes, Sorbonne Paris Cité, Paris, France

Corresponding author: Zhonglin Xie, zxie@gsu.edu, or Ming-Hui Zou, ming-hui-zou@ouhsc.edu.

factor-α (TNF-α) (17). However, the molecular mechanisms by which AMPK suppresses the inflammatory response are incompletely understood. In the current study, we reported that AMPK activation enhances the expression of mitogen-activated protein kinase phosphase-1 (MKP-1), resulting in suppression of STAT1 signaling and inhibition of vascular inflammation. Our studies have established a central role for AMPK in promoting an anti-inflammatory phenotype that is vital for protecting against insulin resistance and limiting the progression of inflammatory vascular diseases.

RESEARCH DESIGN AND METHODS

Human aortic smooth muscle cells (HASMCs) and cell culture media (Medium 231) were purchased from Cascade Biologics (Portland, OR). DMEM/Ham's F12 medium was obtained from Mediatech (Herndon, VA). Phosphorylated (phospho)-STAT1 (Tyr701) antibody, Alexa-Fluor 594 goat anti-rabbit, and Alexa-Fluor 594 goat anti-mouse IgG were purchased from the Invitrogen Corporation (Carlsbad, CA). STAT1 antibody was acquired from Upstate Biotechnology (Lake Placid, NY). Antibodies against phospho-AMPK (Thr172), AMPK, monocyte chemotactic protein-1 (MCP-1), CD45, and the Src homology-2 domain–containing protein tyrosine phosphatase 2 (SHP2) were purchased from Cell Signaling Technology (Beverly, MA). Anti-CD68 antibody was obtained from Abcam (Cambridge, MA). Anti–MKP-1 antibody and MKP-1–specific small interfering (si)RNA duplexes were purchased from Santa Cruz Biotechnology (Santa Cruz, CA). Antibodies against inducible nitric oxide synthase (iNOS) and cyclooxygenase-2 (COX-2) were procured from BD Bioscience (Franklin Lakes, NJ). IFN-γ was purchased from R&D Systems (Minneapolis, MN). AICAR (5-aminoimidazole-4-carboxyamide ribonucleoside) was obtained from Toronto Research Chemicals Inc., and compound C was bought from Calbiochem (San Diego, CA). Fludarabine was obtained from Bosche Scientific (New Brunswick, NJ). Angiotensin II (AngII) and other chemicals, as well as organic solvents of research grade, were purchased from Sigma-Aldrich (St. Louis, MO).

Experimental Animals and Treatments
C57BL/6 (wild-type [WT]), AMPKα1 knockout (AMPKα1$^{-/-}$), and AMPKα2$^{-/-}$ mice were bred at the animal facility of the University of Oklahoma Health Sciences Center. At 8 weeks of age, WT and AMPKα2$^{-/-}$ mice were randomly assigned to receive subcutaneous implantation of a minipump (Model 2004; ALZA Corp., Palo Alto, CA) loaded with AngII (0.7 mg/kg/day) or phosphate buffered saline (PBS) (18). Simultaneously, the mice were assigned to be treated with fludarabine (100 mg/kg, i.p.) or vehicle once every other day (19). After 4 weeks of treatment, blood pressures were measured using Millar Mikro-Tip catheter (Millar Instruments) (20), and aortas were harvested for immunohistochemical and molecular biological analyses. The animal protocol was reviewed and

approved by the University Institutional Animal Care and Use Committee.

Cell Culture
HASMCs were maintained in Medium 231 with Smooth Muscle Growth Supplement. Mouse aortic smooth muscle cells (MASMCs) were isolated from thoracic aortas of WT, AMPKα1$^{-/-}$, and AMPKα2$^{-/-}$ mice, as described previously (21), and were grown in DMEM/F12 medium supplemented with 5% FBS and Smooth Muscle Growth Supplement. All culture media were supplemented with penicillin (100 units/mL) and streptomycin (100 μg/mL). Cultured cells were incubated in a humidified atmosphere of 5% CO_2 and 95% air at 37°C and used between passage 3 and 10.

Adenovirus Infection and siRNA Transfection
Cells were infected with adenovirus encoding AMPK-CA (constitutively active) or AMPK-DN (dominant-negative) at a multiplicity of infection of 50 in medium with 5% FBS for 48 h. An adenovirus encoding green fluorescent protein (Ad-GFP) was used as a control. Under these conditions, infection efficiency was >80%, as determined by measuring GFP expression (22,23). MKP-1 siRNA and control siRNA were obtained from Santa Cruz Biotechnology. HASMCs were transfected with MKP-1 siRNA or control siRNA for 48 h using Lipofectamine RNAiMAX (Invitrogen) according to the manufacturer's instructions (24).

Determination of Cytokines Release
HASMCs and MASMCs were grown in 12-well plates. After the treatment, media were harvested for measurement of IL-6, IL-1β, MCP-1, and TNF-α. The cytokine levels were determined using an ELISA kit (Bio-Rad, Hercules, CA) according to the manufacturer's instructions. The assay selectively recognizes each cytokine with a limit of detection of >3.2 pg/mL.

RNA Isolation and Quantitative Real-Time PCR
Detailed methods are provided in the Supplementary Data.

Western Blot Analysis
Cells and aortic tissues were homogenized in lysis buffer, and the protein content was assayed with bicinchoninic acid protein assay reagent (Pierce, Rockford, IL). Protein (50–80 μg) was resolved by SDS-PAGE, transferred to nitrocellulose membranes, and probed with specific antibodies. The signals were visualized by enhanced chemiluminescence (GE Healthcare), and then the membranes were stripped and probed with total protein and/or β-actin to verify equal loading, as described previously (22, 25,26). The intensity of individual bands was measured by AlphaEase (Alpha Innotech, Santa Clara, CA), and the background was subtracted from the calculated area.

26S Proteasome Activity Assay
26S proteasome activity was assayed by measuring ATP-dependent degradation of proteasome fluorescence substrates, as described previously (27).

Electrophoretic Mobility Shift Assay

Nuclear fractions for the electrophoretic mobility shift assay (EMSA) were prepared using NE-PER Nuclear and Cytoplasmic Extraction Reagents (Pierce) according to the manufacturer's protocol. EMSA was done using a gel shift kit (Panomics) following the manufacturer's instructions. The specificity of binding was verified with an unlabeled consensus oligonucleotide corresponding to the STAT1 binding sequence as a competitor in the binding reaction.

Immunohistochemical Staining and Immunofluorescence Microscopy

The thoracic aortas were fixed in 4% paraformaldehyde, embedded in paraffin, and sectioned at 4 μm. The sections were deparaffinized and stained with vascular cell adhesion molecule 1 (VCAM-1), MCP-1, iNOS, TNF-α, or IL-1β antibodies, as described previously (28).

Statistical Analysis

Data are expressed as mean ± SEM. Statistical differences were analyzed by one-way ANOVA, followed by Bonferroni post hoc analysis, except for the time course data, which were analyzed with repeated-measures ANOVA. Comparisons between the groups were assessed using the Student t test. A value of $P < 0.05$ was considered statistically significant.

RESULTS

Activation of AMPK Suppresses STAT1 in HASMCs

Recent evidence indicates that inhibition of AMPK is involved in the low-grade inflammation found in metabolic syndrome (29). Because STAT1 activation often correlates with cellular proinflammatory activity, we first determined whether AMPK suppresses inflammation through inhibition of STAT1 signaling in HASMCs, because vascular smooth muscle cells (VSMCs) are the main component of the vascular media and the activities of VSMCs are important in normal vascular repair and in pathological processes. HASMCs were incubated with AICAR (2 mmol/L) for the indicated time points, and AMPK activation was determined by evaluating the phosphorylation of AMPK at Thr172. A significant increase in AMPK phosphorylation was observed at 2 h after AICAR treatment and reached a peak at 8 h (Fig. 1A). As a putative target of AMPK, the phosphorylation of STAT1 at Tyr701 started to decline at 2 h after the treatment and remained suppressed at 16 h. AICAR did not change the protein levels of STAT1 (Fig. 1A), suggesting that the alteration in STAT1 phosphorylation was not due to the reduction in STAT1 protein expression. In addition, AICAR increased AMPK Thr172 phosphorylation in a dose-dependent manner, which was paralleled by decreased STAT1 phosphorylation (Fig. 1B). Similarly, activation of AMPK by metformin, another AMPK activator, decreased STAT1 phosphorylation (Supplementary Fig. 1). In contrast to inhibition of STAT1 phosphorylation by AICAR-activated AMPK, compound C, a well-characterized AMPK inhibitor, reduced AMPK phosphorylation and enhanced STAT1 phosphorylation at 20 μmol/L (Fig. 1C). The administration of compound C also increased STAT1 phosphorylation in a time-dependent manner (Fig. 1D).

Once activated, the phospho-STAT proteins translocated to the nucleus, bound to specific promoters, and induced the expression of target genes (30). We therefore determined whether AMPK influences STAT1 subcellular localization. In control HASMCs, the phospho-STAT1 was mainly present in the cytoplasm. Notably, in HASMCs exposed to compound C (20 μmol/L, 16 h) the phospho-STAT1 was mainly detected in the nucleus, suggesting that AMPK inhibition induces STAT1 nuclear translocation (Fig. 1E). We further examined whether AMPK influences the DNA-binding activity of STAT1. As revealed by EMSA, AICAR reduced STAT1 DNA-binding signal intensity, whereas compound C increased the DNA-binding activity of STAT1 (Fig. 1F–H), suggesting that AMPK negatively regulates STAT1 signaling in HASMCs.

AMPK Activation Attenuates IFN-γ–Enhanced STAT1 Activity

The JAK/STAT pathway was initially identified as a primary mediator of intracellular signaling induced by IFN-γ (2). To determine the inhibitory effect of AMPK on STAT1 signaling, we studied whether AMPK activation suppresses IFN-γ–stimulated STAT1 activity. IFN-γ inhibited AMPK, as demonstrated by decreased AMPK phosphorylation, accompanied by increased STAT1 phosphorylation (Fig. 2A). AICAR activated AMPK and markedly attenuated IFN-γ–induced STAT1 phosphorylation (Fig. 2A). Immunocytochemical staining showed that in control and AICAR-treated HASMCs, the phospho-STAT1 was mainly present in the cytoplasm. IFN-γ enhanced the fluorescence intensity of phospho-STAT1 in the nucleus, indicating the nuclear translocation of phospho-STAT1. Administration of AICAR ameliorated this nuclear translocation (Fig. 2B).

AMPK Activation Inhibits AngII-Induced Cytokine Expression

AngII induces vascular inflammation by activating the JAK/STAT cascade and increasing the production of inflammatory cytokines (31). We therefore studied whether AMPK activation could prevent the proinflammatory actions of AngII in cultured HASMCs. Administration of AngII inhibited AMPK phosphorylation along with increased STAT1 phosphorylation and nuclear translocation (Fig. 2C and D). Notably, activation of AMPK by AICAR prevented AngII-enhanced STAT1 phosphorylation and nuclear translocation (Fig. 2C and D). Quantitative analyses of inflammatory cytokine contents in conditioned media revealed that AngII significantly upregulated the production of inflammatory cytokines, including IL-6 and MCP-1 (Fig. 2E and F). AICAR treatment diminished AngII-induced production of proinflammatory cytokines (Fig. 2E and F).

AMPK Activation Increased MKP-1 Protein Levels in VSMCs

STAT1 dephosphorylation by protein phosphatases such as MKP-1 and SHP2 are critical in the regulation of STAT1 activity (32). To gain insight into the mechanism mediating the inhibitory effect of AMPK on the STAT1
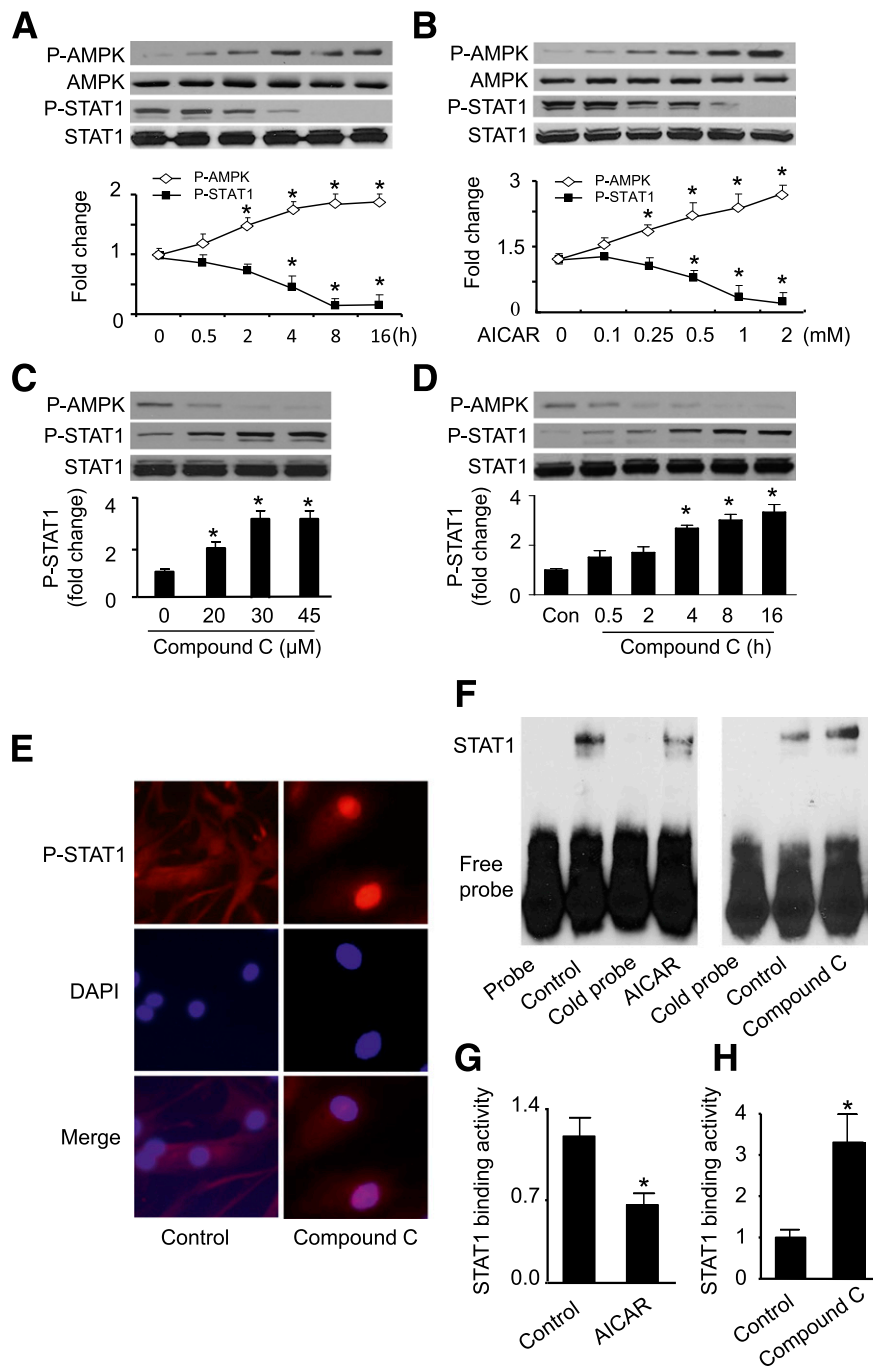
Figure 1—AMPK activation inhibits STAT1 signaling in HASMCs. *A*: Confluent HASMCs were treated with AICAR (2 mmol/L) at the indicated time points. Phosphorylated AMPK at Thr172 (P-AMPK) and phosphorylated STAT1 at Tyr701 (P-STAT1) in cell lysates were analyzed by Western blotting. *B*: HASMCs were treated with varying concentrations of AICAR for 16 h. Cell lysates were subjected to Western analysis of P-AMPK and P-STAT1. *C*: Phosphorylation of AMPK and STAT1 was detected in HASMCs treated with indicated concentrations of compound C for 16 h. *D*: STAT1 and AMPK phosphorylation in response to compound C (20 μmol/L) was measured by Western blotting ($n = 4$). *$P < 0.05$ vs. control (Con). *E*: Immunofluorescence staining of P-STAT1 in HASMCs treated with or without compound C. The photographs are representative of three independent experiments. *F*: HASMCs were treated with AICAR (2 mmol/L) or compound C (20 μmol/L) for 16 h, and DNA-binding activity of STAT1 was determined by EMSA. *G* and *H*: Densitometric analysis of STAT1 DNA-binding activity ($n = 4$). *$P < 0.05$ vs. control.

pathway, we determined whether AMPK regulates the expression of protein phosphatases. Activation of AMPK by AICAR or overexpression of AMPK-CA adenovirus enhanced MKP-1 protein levels, whereas inhibition of

AMPK by compound C or AMPK-DN adenovirus reduced MKP-1 protein expression (Fig. 3*A* and *B*). Moreover, deletion of AMPKα1 or AMPKα2 in MASMCs reduced MKP-1 protein levels (Supplementary Fig. 2*A*). We also examined
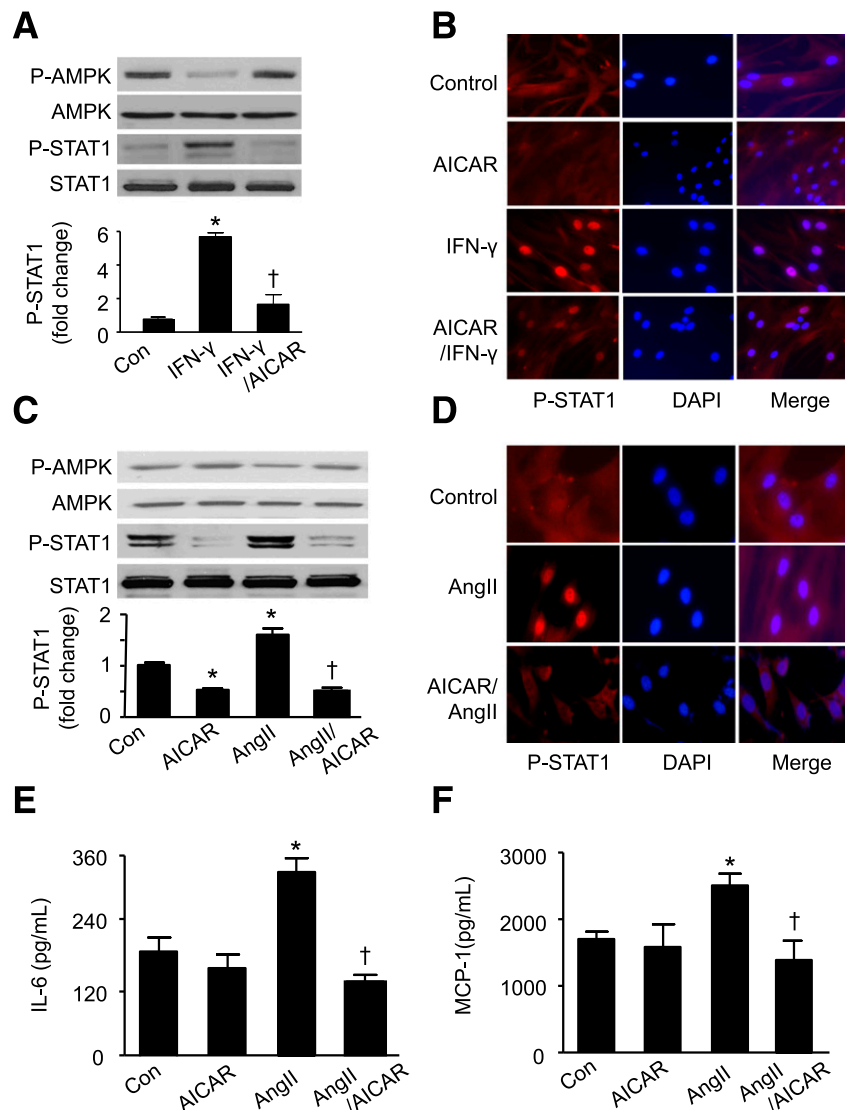
Figure 2—AICAR treatment attenuates IFN-γ–enhanced STAT1 activity and suppresses AngII-induced proinflammatory cytokine expression. A: HASMCs were pretreated with AICAR (2 mmol/L) for 16 h and then treated with IFN-γ (100 ng/mL) for 30 min. Phosphorylation of AMPK (P-AMPK) and STAT1 (P-STAT1) was examined by Western blotting (n = 3). *P < 0.05 vs. control; †P < 0.05 vs. IFN-γ. B: Subcellular distribution of P-STAT1 was determined by immunocytochemistry. The photographs are representative of three independent experiments. C: After being treated with AICAR for 16 h, HASMCs were treated with or without AngII (1 μmol/L) for 24 h. AMPK and STAT1 phosphorylation were measured by Western blotting. D: Subcellular distribution of P-STAT1 was determined by immunocytochemistry. The photographs are representative of three independent experiments. E and F: HASMCs were treated with or without AngII (1 μmol/L) for 24 h after being treated with AICAR for 16 h. IL-6 and MCP-1 in conditioned media were measured by ELISA (n = 4).*P < 0.05 vs. control (Con); †P < 0.05 vs. AngII.

the effect of AMPK on SHP2, another protein phosphatase that had been reported to dephosphorylate STAT1. Neither activation of AMPK by AICAR and metformin nor inhibition of AMPK by genetic deletion of AMPK and administration of compound C altered SHP2 expression (Supplementary Fig. 2B), indicating that AMPK activation increases MKP-1 protein expression in VSMCs.

Inhibition of STAT1 Phosphorylation by AMPK Is MKP-1 Dependent

Induction of MKP-1 has been demonstrated to inhibit STAT1 phosphorylation in AngII-activated VSMCs (33)

and to reduce STAT1 activity in macrophages (34). We therefore determined whether AMPK regulates STAT1 phosphorylation through MKP-1 via genetic means. Transfection of MASMCs isolated from WT, AMPKα1$^{-/-}$, and AMPKα2$^{-/-}$ mice with Ad-MKP-1 resulted in higher expression of MKP-1, whereas Ad-GFP did not. The increase in MKP-1 protein levels abolished AMPK-deficiency–enhanced STAT1 phosphorylation (Fig. 3C). Conversely, transfection of HASMCs with MKP-1 siRNA significantly reduced MKP-1 protein levels, which were associated with an increase in STAT1 phosphorylation (Fig. 3D). In addition, overexpression of AMPK-CA enhanced MKP-1 levels
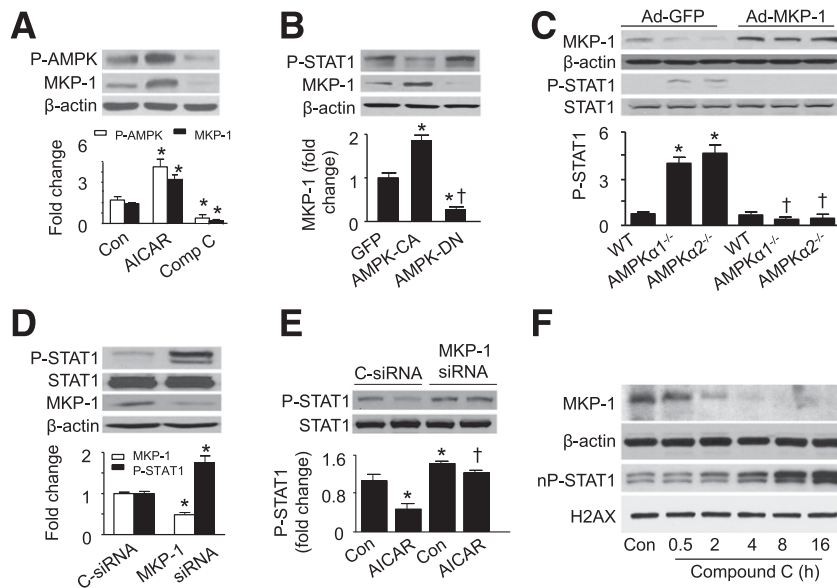
Figure 3—MKP-1 mediates suppression of STAT1 by AMPK. *A*: Confluent HASMCs were treated with AICAR (2 mmol/L) for 4 h or compound C (Comp C) for 8 h. AMPK phosphorylation (P-AMPK) and MKP-1 protein levels were detected by Western blotting ($n = 5$). *$P < 0.05$ AICAR vs. control (Con). *B*: HASMCs were transfected with GFP, AMPK-CA, or AMPK-DN adenovirus for 48 h. STAT1 phosphorylation (P-STAT1) and MKP-1 protein levels were detected by Western blotting ($n = 4$).*$P < 0.05$ vs. GFP; †$P < 0.05$ vs. AMPK-CA. *C*: WT and AMPK-deficient MASMCs were transfected with adenovirus encoding GFP (Ad-GFP) or MKP-1 (Ad-MKP-1) for 48 h. MKP-1 protein levels and STAT1 phosphorylation were determined by Western blotting ($n = 3$).*$P < 0.05$ vs. WT/GFP; †$P < 0.05$ AMPK$\alpha 1^{-/-}$ and AMPK$\alpha 2^{-/-}$ plus Ad-GFP vs. AMPK$\alpha 1^{-/-}$ and AMPK$\alpha 2^{-/-}$ plus Ad-MKP-1. *D*: MKP-1 protein levels and STAT1 and P-STAT1 were analyzed by Western blotting in HASMCs transfected with control (C)-siRNA or MKP-1 siRNA ($n = 3$). *$P < 0.05$ vs. C-siRNA. *E*: HASMCs were transfected with C-siRNA or MKP-1 siRNA for 48 h and then treated with AICAR (2 mmol/L) for 4 h. Cell lysates were subjected to Western analysis of STAT1 phosphorylation ($n = 3$). *$P < 0.05$ vs. C-siRNA; †$P < 0.05$ vs. AICAR/C-siRNA. *F*: HASMCs were treated with compound C (20 μmol/L) for the indicated time points. MKP-1 protein levels in cell lysates and P-STAT1 in nuclear (n) fractions were analyzed by Western blotting. Histone H2AX was used as a loading control for nuclear fractions.

and reduced STAT1 phosphorylation, whereas overexpression of AMPK-DN adenovirus had opposite effects (Fig. 3*B*). The reduction in MKP-1 expression by MKP-1 siRNA prevented AICAR-reduced STAT1 phosphorylation (Fig. 3*E*).

We showed that compound C treatment time-dependently reduced AMPK phosphorylation with a concomitant increase in STAT1 phosphorylation (Fig. 1*D*). To determine the role of AMPK in regulating the MKP-1–STAT1 signaling pathway, we further examined the sequential alterations in MKP-1 protein expression and STAT1 nuclear translocation. As AMPK phosphorylation decreased (Fig. 1*D*), MKP-1 protein levels gradually declined (Fig. 3*F*). At the same time, STAT1 phosphorylation (Fig. 1*D*) and its nuclear translocation increased (Fig. 3*F*). These data suggest that AMPK activation suppresses STAT1 signaling through upregulation of MKP-1.

Deletion of AMPK Reduces MKP-1 Protein Levels by Increasing Proteasome-Mediated Degradation of MKP-1

Because MKP-1 was rapidly degraded by proteasome after induction (32,35) and AMPK activation inhibited proteasome activity (27,36), we investigated whether AMPK increases MKP-1 protein levels by inhibiting proteasome-dependent

degradation of MKP-1. We found that activation of AMPK by AICAR reduced 26S proteasome activity in cultured HASMCs (Fig. 4*A*), which was accompanied by an increase in MKP-1 protein levels (Fig. 4*B*). However, AICAR treatment had no effect on MKP-1 mRNA expression (Fig. 4*C*). We next studied whether deletion of AMPK reduces MKP-1 protein levels by increasing proteasome-mediated degradation of MKP-1 in WT, AMPK$\alpha 1^{-/-}$, and AMPK$\alpha 2^{-/-}$ MASMCs. Deletion of AMPK$\alpha 1$ or AMPK$\alpha 2$ caused an increase in 26S proteasome activity. Administration of MG-132, a potent proteasome inhibitor, suppressed proteasome activity in WT and AMPK-deficient MASMCs (Fig. 4*D*). Consistent with the alterations in proteasome activity, AMPK-deficient MASMCs had lower levels of MKP-1 protein than did WT MASMCs. The administration of MG-132 significantly increased MKP-1 protein levels in WT and AMPK-deficient MASMCs (Fig. 4*E*). These data indicated that deletion of AMPK enhanced proteasome-mediated degradation of MKP-1.

AMPK Deficiency Increases STAT1 Activity in MASMCs

To establish the inhibitory effect of AMPK on vascular inflammation, we further tested our hypothesis in AMPK-deficient MASMCs. Compared with WT MASMCs, AMPK$\alpha 1^{-/-}$ and AMPK$\alpha 2^{-/-}$ MASMCs had higher levels
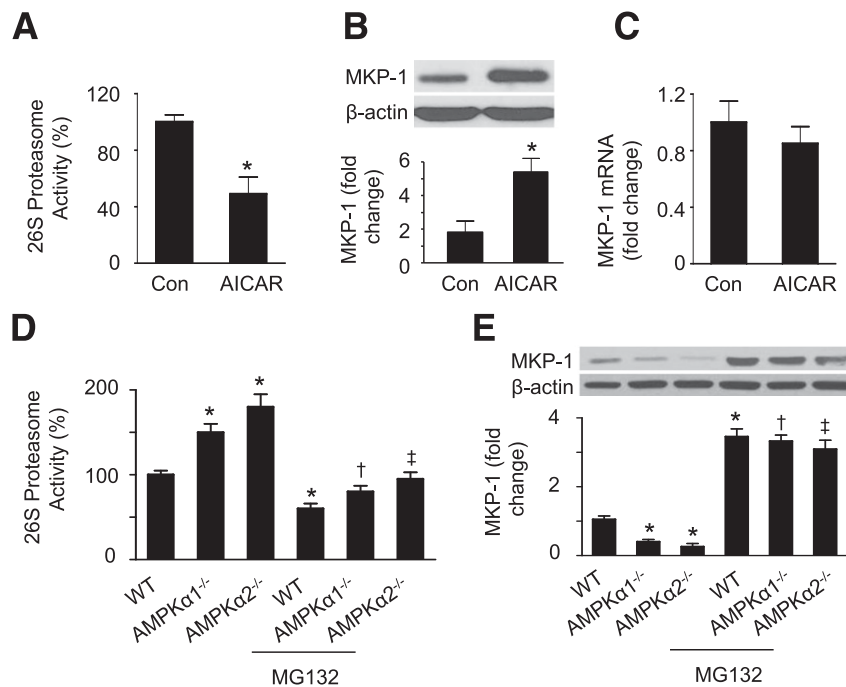
Figure 4—Deletion of AMPK reduces MKP-1 protein levels by increasing proteasome-mediated degradation of MKP-1. *A*: HASMCs were treated with AICAR (2 mmol/L) for 4 h. The activity of 26*S* proteasome in cell lysates was assayed as described in RESEARCH DESIGN AND METHODS. *B*: MKP-1 protein levels were detected by Western blotting (*n* = 5). *P < 0.05 vs. control (Con). *C*: MKP-1 mRNA was measured by quantitative real-time PCR (*n* = 5). *D*: WT and AMPK-deficient MASMCs were treated with or without MG-132 (0.5 μmol/L) for 4 h. The activity of 26*S* proteasome in cell lysates was detected (*n* = 4). *P < 0.05 vs. WT control; †P < 0.05 vs. AMPKα1$^{-/-}$; ‡P < 0.05 vs. AMPKα2$^{-/-}$. *E*: MKP-1 protein levels were determined by Western blotting (*n* = 4). *P < 0.05 vs. WT control; †P < 0.05 vs. AMPKα1$^{-/-}$; ‡P < 0.05 vs. AMPKα2$^{-/-}$.

of phospho-STAT1 (Fig. 5*A*). Immunocytochemical staining of phospho-STAT1 revealed that phospho-STAT1 was mainly present in the cytoplasm in WT MASMCs but translocated into the nucleus in AMPKα1$^{-/-}$ and AMPKα2$^{-/-}$ MASMCs (Fig. 5*B*). Consistently, gel shift assay showed that the DNA-binding activity of STAT1 was increased in AMPKα1$^{-/-}$ and AMPKα2$^{-/-}$ MASMCs compared with WT MASMCs (Fig. 5*C* and *D*). To determine the specificity of the interaction, anti-STAT1 antibody was added to the reaction mixtures. The addition of anti-STAT1 antibody, but not IgG, prevented the interaction between STAT1 and DNA (Fig. 4*E*).

Inhibition of STAT1 Attenuates AMPK-Deficiency–Enhanced Inflammatory Mediators in MASMCs

We next examined whether AMPK-mediated STAT1 inhibition results in the suppression of inflammatory response by measuring the production of inflammatory mediators in MASMCs transfected with control or STAT1 siRNA. Western blot analysis revealed a significant reduction of STAT1 expression in the MASMCs transfected with STAT1 siRNA compared with the cells transfected with control siRNA (Fig. 5*A*). The downregulation of STAT1 reduced STAT1 phosphorylation in AMPKα1$^{-/-}$ and AMPKα2$^{-/-}$ MASMCs (Fig. 6*A*). The expression of iNOS and COX-2 was increased in AMPKα1$^{-/-}$ and AMPKα2$^{-/-}$ MASMCs. The increase in iNOS and COX-2

expression was diminished by knockdown of STAT1 (Fig. 6*B*).

To augment the results obtained by genetic inhibition of STAT1, we investigated whether AMPK suppresses vascular inflammation through inhibition of STAT1 using a pharmacologic inhibitor, fludarabine, which has been reported to specifically inhibit STAT1 in peripheral blood mononuclear cells and VSMCs (37,38). Consistent with previous findings, fludarabine treatment significantly prevented STAT1 phosphorylation in AMPK-deficient MASMCs. As a result, the increased expression of iNOS and COX-2 in AMPKα1$^{-/-}$ and AMPKα2$^{-/-}$ MASMCs was abolished by fludarabine treatment (Fig. 6*C* and *D*). We further quantified IL-1β, TNF-α, IL-6, and MCP-1 levels in conditioned media. IL-1β and TNF-α levels were undetectable in the conditioned media (data not shown). Deletion of AMPKα1 or AMPKα2 enhanced IL-6 and MCP-1 levels by 10-fold in the conditioned media, and the inhibition of STAT1 by fludarabine diminished the secretion of IL-6 and MCP-1 (Fig. 6*E* and *F*).

Deletion of AMPKα2$^{-/-}$ Reduces MKP-1 Protein Levels and Enhances STAT1 Phosphorylation in Mouse Aortas

The catalytic α subunit of AMPK has two isoforms, α1 and α2. Knockout of either the α1 or α2 subunit results in visually normal mice, but knockout of both α1 and α2
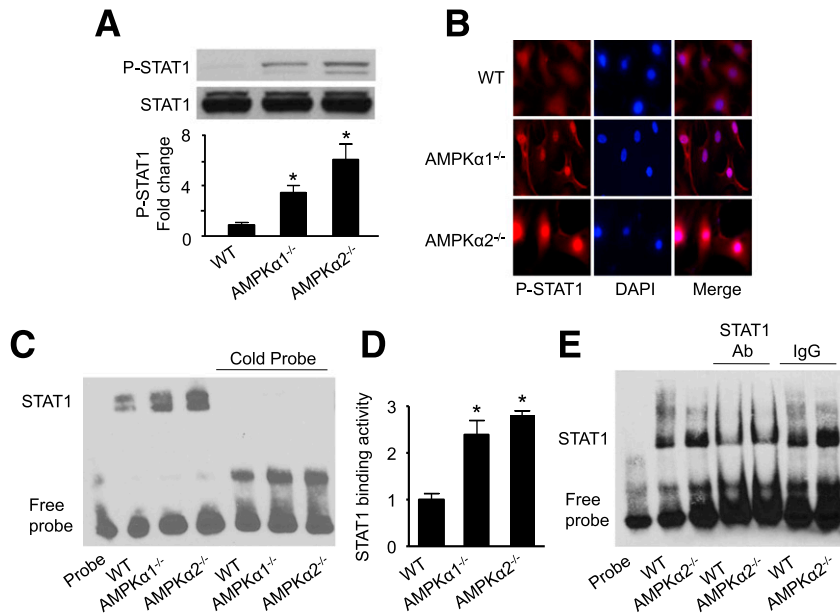
Figure 5—Deletion of AMPK increases STAT1 phosphorylation, nuclear translocation, and DNA-binding activity in MASMCs. *A*: MASMCs were isolated from WT, AMPKα1$^{-/-}$, or AMPKα2$^{-/-}$ mice, and cell lysates were subjected to Western blot to determine the phosphorylation of STAT1 (P-STAT1) (*n* = 4). *P < 0.05 vs. WT. *B*: Subcellular distribution of P-STAT1 was determined by immunocytochemistry. The photographs are representative of three independent experiments. *C*: DNA-binding activity of STAT1 was measured by EMSA. *D*: Densitometric analysis of STAT1 DNA-binding activity (*n* = 4). *P < 0.05 vs. WT. *E*: Anti-STAT1 antibody was added to the reaction mixtures to test the specificity of the interaction.

subunits is lethal at around embryonic day 9.5 (24), showing that the α1 and α2 subunits have compensatory roles in regulating fetal growth and development. AMPKα1 and AMPKα2 seem to be equally important in maintaining vascular function. Using AMPKα2$^{-/-}$ mice, we have shown that reduction of AMPKα2 activates NF-κb and increases atherosclerosis in vivo (27,39). Thus, we used these mice to determine the mechanisms underlying the anti-inflammatory effect of AMPK in vivo. AngII is a proinflammatory peptide (40) and contributes to diabetes-induced vascular inflammation (41). Therefore, we infused WT and AMPKα2$^{-/-}$ mice with AngII (0.7 mg/kg/day) for 4 weeks (18). We first determined the effect of AngII on blood pressure in these mice. Deletion of AMPKα2 significantly increased mean blood pressure (WT, 80.1 ± 3; AMPKα2$^{-/-}$, 117 ± 6 mmHg; *P* < 0.05). AngII infusion did not significantly increase mean blood pressure in WT (control, 80.1 ± 3; AngII, 86.1 ± 8 mmHg; *P* = NS) and AMPKα2$^{-/-}$ (control, 117 ± 6; AngII, 125 ± 7; *P* = NS) mice.

Next, we examined MKP-1 protein levels and STAT1 phosphorylation by Western blotting and immunohistochemistry. Consistent with the findings in cultured aortic smooth muscle cells, deletion of AMPKα2 significantly reduced MKP-1 protein levels in mouse aortas. AngII infusion reduced MKP-1 protein levels in WT mice and led to a further decrease in MKP-1 protein levels in AMPKα2$^{-/-}$ mice. Using the STAT1 inhibitor fludarabine did not affect the expression of MKP-1 in WT and AMPKα2$^{-/-}$ mice under basal and AngII-infusion conditions

(Fig. 7*A* and *B*). Consistent with the change in MKP-1 protein levels, AMPKα2$^{-/-}$ mice exhibited higher levels of phospho-STAT1. Chronic infusion of AngII enhanced the expression of phospho-STAT1 in WT mice, and the effect was exaggerated in AMPKα2$^{-/-}$ mice. Fludarabine treatment significantly reduced STAT1 phosphorylation in WT and AMPKα2$^{-/-}$ mice (Fig. 7*C* and *D*).

Deletion of AMPKα2 Exacerbates the Inflammatory Response in Mouse Aortas

We further evaluated inflammatory cell infiltration in mouse aortas using antibodies against CD68 and CD45 as markers for macrophages (Fig. 8*A*) and leukocytes (Supplementary Fig. 3), respectively (42). In WT mice, AngII infusion increased CD68 and CD45 expression. Fludarabine treatment attenuated AngII-induced macrophage and leukocyte infiltration. In AMPKα2$^{-/-}$ mouse aortas, AngII infusion induced more macrophage and leukocyte infiltration compared with WT mouse aortas; the infiltration was also reduced by fludarabine treatment (Fig. 8*A* and Supplementary Fig. 3).

To establish the role of AMPK in the suppression of vascular inflammation in vivo, the expression of proinflammatory mediators in aortas was evaluated at mRNA and protein levels using quantitative real-time PCR and immunohistochemistry, respectively. In WT mice, AngII infusion increased VCAM-1 (Fig. 8*B*), MCP-1 (Fig. 8*C*), iNOS (Fig. 8*D*), TNF-α (Fig. 8*E*), and IFN-γ (Fig. 8*F*) expression at protein and mRNA levels. The increases were reduced by fludarabine therapy (Fig. 8*B–F*). Compared
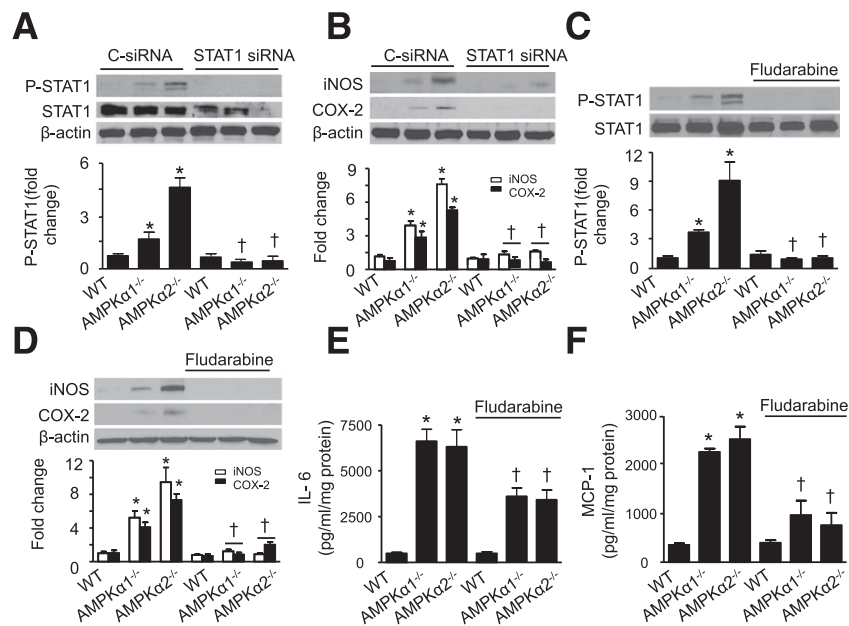
Figure 6—STAT1 inhibition attenuates expression of inflammatory mediators in AMPK-deficient MASMCs. *A*: MASMCs were transfected with control (C)-siRNA or STAT1 siRNA for 48 h. STAT1 phosphorylation (P-STAT1) was evaluated by Western blotting. *B*: Protein levels of iNOS and COX-2 were analyzed by Western blotting ($n = 3$). *$P < 0.05$ vs. WT; †$P < 0.05$ AMPKα1$^{-/-}$ and AMPKα2$^{-/-}$ vs. AMPKα1$^{-/-}$ and AMPKα2$^{-/-}$ plus STAT1 siRNA. *C*: MASMCs were treated with fludarabine (50 μmol/L) for 16 h, and P-STAT1 was determined by Western blotting. *D*: Western blot analysis was used to determine the expression of iNOS and COX-2 in cell lysates ($n = 4$). *$P < 0.05$ vs. WT; †$P < 0.05$ AMPKα1$^{-/-}$ and AMPKα2$^{-/-}$ vs. AMPKα1$^{-/-}$ and AMPKα2$^{-/-}$ plus fludarabine. IL-6 (*E*) and MCP-1 protein (*F*) levels in conditioned media from WT and AMPK-deficient MASMCs were determined by ELISA ($n = 3$). *$P < 0.05$ vs. WT; †$P < 0.05$ AMPKα1$^{-/-}$ and AMPKα2$^{-/-}$ vs. AMPKα1$^{-/-}$ and AMPKα2$^{-/-}$ plus fludarabine.

with WT conditions, deletion of AMPKα2 increased the expression of VCAM-1 (Fig. 8*B*), iNOS (Fig. 8*D*), TNF-α (Fig. 8*E*), and IFN-γ (Fig. 8*F*), and amplified AngII-enhanced expression of inflammatory cytokines (VCAM-1, MCP-1, iNOS, TNF-α, and IFN-γ) at protein and mRNA levels (Fig. 8*B*–*F*). Fludarabine treatment attenuated the AngII-induced expression of inflammatory cytokines in AMPKα2$^{-/-}$ mice (Fig. 8*B*–*F*).

DISCUSSION

Type 2 diabetes is characterized by chronic inflammation, suppression of AMPK activity, and acceleration of atherosclerosis. However, the mechanisms by which AMPK inhibition accelerates the inflammatory response remain elusive. In the current study, we found that AMPK deletion promoted proteasome-dependent degradation of MKP-1, activated the STAT1 cascade, enhanced proinflammatory mediator production, and exacerbated AngII-induced vascular inflammation. Conversely, AMPK activation enhanced MKP-1 protein levels, which inhibited the STAT1 signaling pathway, resulting in the suppression of vascular inflammation. These data suggest that AMPK negatively regulates the STAT1 signaling pathway to inhibit vascular inflammation, acting as a crucial regulator of the metabolic pathways governing inflammation.

To examine whether a reduction in AMPK is associated with the switch to a proinflammatory phenotype, we demonstrated that AMPK inhibition activated STAT1

signaling along with the upregulation of proinflammatory mediators. AMPKα2 deletion induced a vascular inflammatory response under basal conditions and aggravated vascular inflammation after AngII infusion. Pharmacological (fludarabine) or genetic (STAT1 siRNA) inhibition of STAT1 reversed the inflammatory phenotype in AMPK-deficient MASMCs and prevented the exacerbated vascular inflammation seen in AMPKα2$^{-/-}$ mice. Although several reports show that AICAR-activated AMPK is associated with COX-2 induction, Chang et al. (43) considered that AICAR may induce COX-2 expression via an AMPK-independent mechanism (43). Taken together, our data suggest that AMPK suppression activates STAT1 signaling, resulting in aberrant inflammation in the vasculature and establishing an essential role for AMPK in promoting an anti-inflammatory phenotype that is vital for protecting against insulin resistance and cardiovascular diseases.

Studies using astrocytes suggested that AMPK does not affect STAT1 phosphorylation but attenuates nuclear translocation, DNA biding, and subsequent gene expression (44). In contrast, our work demonstrated that STAT1 phosphorylation significantly increases in AMPK-deficient MASMCs. Consistent with our findings, AMPK was reported to inhibit monocyte-to-macrophage differentiation (45) and prevent the IL-6–stimulated inflammatory response by suppressing STAT3 phosphorylation (46). The reason for this discrepancy is unclear but
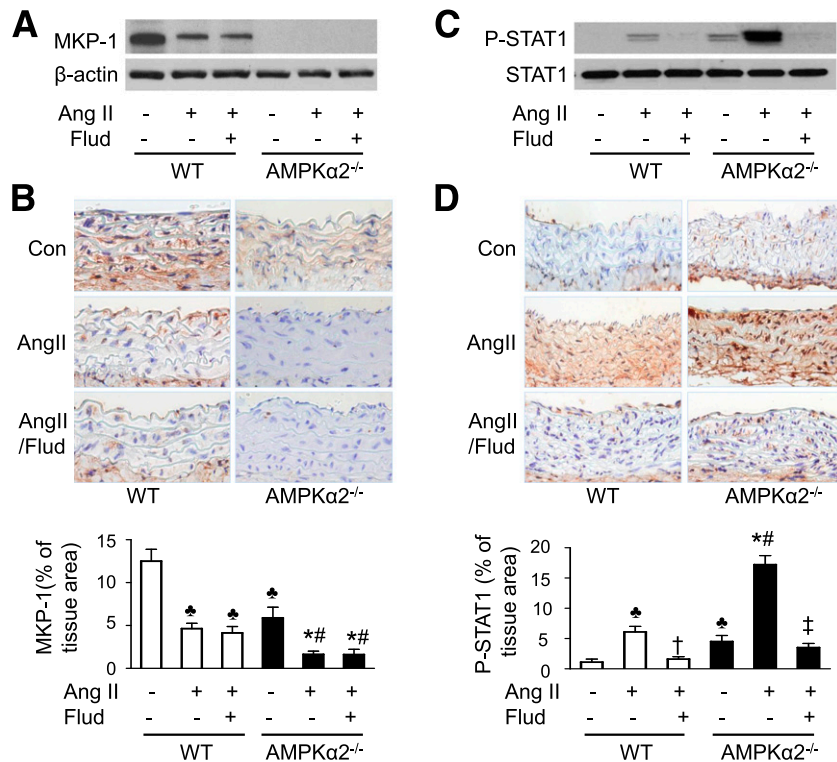
Figure 7—Deletion of AMPKα2 reduces MKP-1 protein levels and enhances STAT1 phosphorylation in mouse aortas. *A*: Protein levels of MKP-1 in mouse aortas were measured by Western blotting. *B*: Aorta sections were stained with MKP-1 antibody, and the stained area was quantified. The photomicrographs are representative of five independent mouse aortas. *C*: STAT1 phosphorylation (P-STAT1) in mouse aortas was measured by Western blotting. *D*: Aorta sections were stained with P-STAT1 antibody, and the stained areas were quantified and expressed as a percentage of total tissue area. ♣$P < 0.05$ vs. WT control; †$P < 0.05$ vs. WT/AngII; *$P < 0.05$ vs. AMPKα2$^{-/-}$/control; #$P < 0.05$ AMPKα2$^{-/-}$/AngII vs. WT/AngII; ‡$P < 0.05$ vs. AMPKα2$^{-/-}$/AngII. Flud, fludarabine.

may be related to the different cell types used in the studies.

Our results suggest that MKP-1 mediates the regulatory effect of AMPK on STAT1 activity. Although MKP-1 overexpression does not reduce tyrosine phosphorylation of STAT1 in COS-1 cells (47), several studies indicate that MKP-1 is a negative regulator of STAT1 in macrophages and VSMCs. In macrophages, global knockout or gene silencing of MKP-1 significantly enhances and prolongs the STAT1 phosphorylation induced by lipopolysaccharides (34,48). Further, MKP-1 antisense oligonucleotide increases STAT1 phosphorylation under basal conditions and prevents AngII-induced STAT1 phosphorylation (33). These data suggest that MKP-1 may be the phosphatase responsible for STAT1 dephosphorylation and inactivation in VSMCs. In support of this model, we have demonstrated that gene silencing of MKP-1 markedly increased STAT1 phosphorylation and prevented AICAR-reduced STAT1 phosphorylation. Taken together, our results suggest that MKP-1 mediates the inhibitory effect of AMPK on STAT1 signaling by reducing STAT1 phosphorylation, thus playing a critical role in inhibiting vascular inflammation.

MKP-1 is a labile protein and is targeted for degradation by the proteasome machinery (35). Diabetes has been documented to increase proteasome activity (49) and reduce MKP-1 protein levels in diabetic animals (50), suggesting that diabetes may increase the degradation of MKP-1 by enhancing proteasome activity. In endothelial cells, deletion of AMPKα2 is associated with an increase in 26S proteasome activity (27). Consistently, we also found that activation of AMPK by AICAR reduced 26S proteasome activity and enhanced MKP-1 protein levels in VSMCs, whereas deletion of AMPK has the opposite effect. Further, administration of MG-132, a potent proteasome inhibitor, dramatically increased MKP-1 protein levels in WT and AMPK-deficient mouse aortic endothelial cells, suggesting that AMPK increases MKP-1 protein levels by inhibiting proteasome-dependent degradation of MKP-1.

In summary, AMPK suppression enhances proteasome-dependent degradation of MKP-1, resulting in STAT1 activation and aberrant vascular inflammation. Because AMPK activation mediates an anti-inflammatory phenotype, the AMPK–MKP-1–STAT1 pathway may be a valid pharmacological target for treating inflammation-related diseases such as metabolic syndrome, insulin resistance, and cardiovascular diseases. A further understanding of how AMPK inhibits inflammation in obese individuals and patients with type 2 diabetes holds promise for
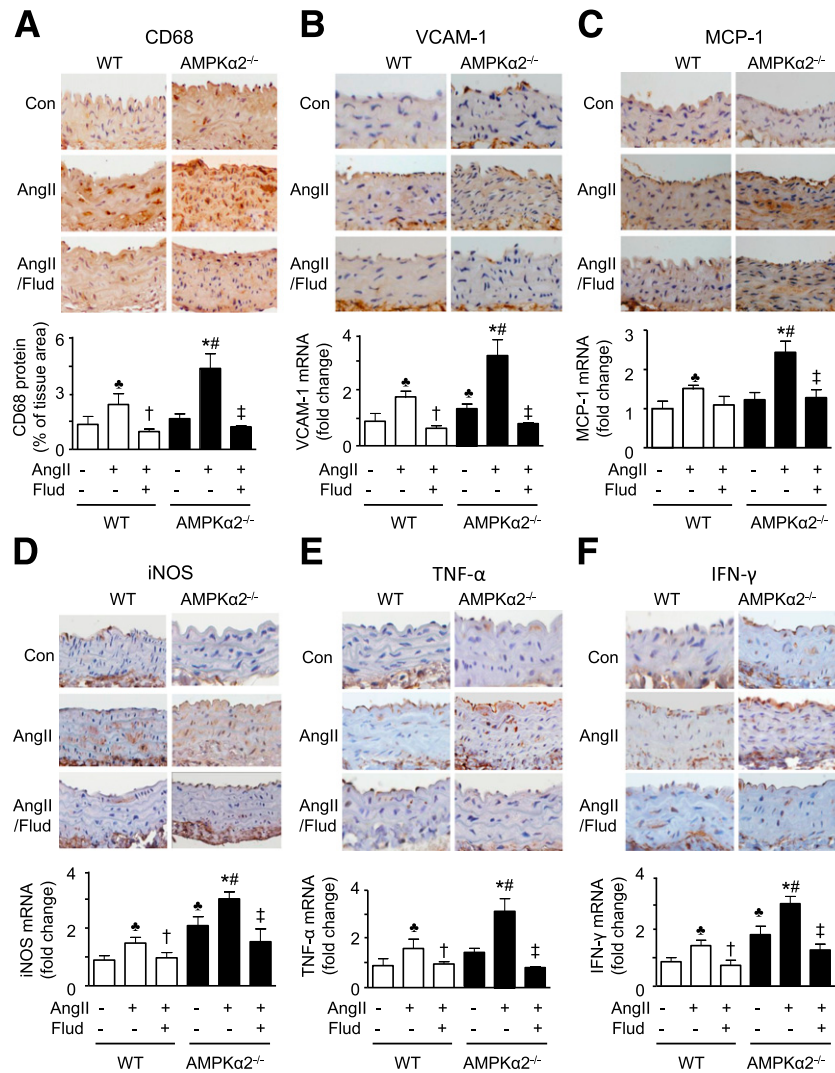
Figure 8—Inhibition of STAT1 by fludarabine (Flud) attenuates AngII-enhanced inflammatory response in WT and AMPKα2$^{-/-}$ mice. *A*: Aorta sections were stained with CD68 antibody and the stained areas were quantified and expressed as a percentage of total tissue area. Expression of VCAM-1 (*B*), MCP-1 (*C*), iNOS (*D*), TNF-α (*E*), and IFN-γ (*F*) was analyzed by using immunohistochemistry. The photomicrographs are representative of five independent mouse aortas. Total RNA were extracted from mouse aortas, and mRNA levels of VCAM-1 (*B*), MCP-1 (*C*), iNOS (*D*), TNF-α (*E*), and IFN-γ (*F*) were determined by quantitative real-time PCR. ♣$P < 0.05$ vs. WT control; †$P < 0.05$ vs. WT/AngII; *$P < 0.05$ vs. AMPKα2$^{-/-}$/control; #$P < 0.05$ AMPKα2$^{-/-}$/AngII vs. WT/AngII; ‡$P < 0.05$ vs. AMPKα2$^{-/-}$/AngII.

identifying new therapies and tailoring current therapies for the prevention and treatment of metabolic and cardiovascular diseases.

References

1. Steinberg GR, Schertzer JD. AMPK promotes macrophage fatty acid oxidative metabolism to mitigate inflammation: implications for diabetes and cardiovascular disease. Immunol Cell Biol 2014;92:340–345

2. Ihle JN. STATs: signal transducers and activators of transcription. Cell 1996; 84:331–334

3. Wunderlich CM, Hövelmeyer N, Wunderlich FT. Mechanisms of chronic JAK-STAT3-SOCS3 signaling in obesity. JAKSTAT 2013;2:e23878

4. Recio C, Oguiza A, Lazaro I, Mallavia B, Egido J, Gomez-Guerrero C. Suppressor of cytokine signaling 1-derived peptide inhibits Janus kinase/signal transducers and activators of transcription pathway and improves inflammation and atherosclerosis in diabetic mice. Arterioscler Thromb Vasc Biol 2014;34:1953–1960

5. Manea A, Tanase LI, Raicu M, Simionescu M. Jak/STAT signaling pathway regulates nox1 and nox4-based NADPH oxidase in human aortic smooth muscle cells. Arterioscler Thromb Vasc Biol 2010;30:105–112

6. Seki Y, Kai H, Shibata R, et al. Role of the JAK/STAT pathway in rat carotid artery remodeling after vascular injury. Circ Res 2000;87:12–18

7. Recinos A 3rd, LeJeune WS, Sun H, et al. Angiotensin II induces IL-6 expression and the Jak-STAT3 pathway in aortic adventitia of LDL receptor-deficient mice. Atherosclerosis 2007;194:125–133

8. Ross R. Atherosclerosis—an inflammatory disease. N Engl J Med 1999;340:115–126

9. Agrawal S, Febbraio M, Podrez E, Cathcart MK, Stark GR, Chisolm GM. Signal transducer and activator of transcription 1 is required for optimal foam cell formation and atherosclerotic lesion development. Circulation 2007;115:2939–2947

10. Hardie DG, Scott JW, Pan DA, Hudson ER. Management of cellular energy by the AMP-activated protein kinase system. FEBS Lett 2003;546:113–120

11. He C, Zhu H, Li H, Zou MH, Xie Z. Dissociation of Bcl-2-Beclin1 complex by activated AMPK enhances cardiac autophagy and protects against cardiomyocyte apoptosis in diabetes. Diabetes 2013;62:1270–1281

12. Xie Z, Lau K, Eby B, et al. Improvement of cardiac functions by chronic metformin treatment is associated with enhanced cardiac autophagy in diabetic OVE26 mice. Diabetes 2011;60:1770–1778

13. Zou MH, Xie Z. Regulation of interplay between autophagy and apoptosis in the diabetic heart: new role of AMPK. Autophagy 2013;9:624–625

14. Ouyang C, You J, Xie Z. The interplay between autophagy and apoptosis in the diabetic heart. J Mol Cell Cardiol 2014;71:71–80

15. Luo Z, Saha AK, Xiang X, Ruderman NB. AMPK, the metabolic syndrome and cancer. Trends Pharmacol Sci 2005;26:69–76

16. Sag D, Carling D, Stout RD, Suttles J. Adenosine 5′-monophosphate-activated protein kinase promotes macrophage polarization to an anti-inflammatory functional phenotype. J Immunol 2008;181:8633–8641

17. Su RY, Chao Y, Chen TY, Huang DY, Lin WW. 5-Aminoimidazole-4-carboxamide riboside sensitizes TRAIL- and TNFalpha-induced cytotoxicity in colon cancer cells through AMP-activated protein kinase signaling. Mol Cancer Ther 2007;6:1562–1571

18. Cassis LA, Gupte M, Thayer S, et al. ANG II infusion promotes abdominal aortic aneurysms independent of increased blood pressure in hypercholesterolemic mice. Am J Physiol Heart Circ Physiol 2009;296:H1660–H1665

19. Jones OY, Alexander PJ, Lacson A, et al. Effects of fludarabine treatment on murine lupus nephritis. Lupus 2004;13:912–916

20. Xie Z, Singh M, Singh K. Osteopontin modulates myocardial hypertrophy in response to chronic pressure overload in mice. Hypertension 2004;44:826–831

21. Kobayashi M, Inoue K, Warabi E, Minami T, Kodama T. A simple method of isolating mouse aortic endothelial cells. J Atheroscler Thromb 2005;12:138–142

22. Xie Z, Dong Y, Zhang J, Scholz R, Neumann D, Zou MH. Identification of the serine 307 of LKB1 as a novel phosphorylation site essential for its nucleocytoplasmic transport and endothelial cell angiogenesis. Mol Cell Biol 2009;29:3582–3596

23. Xie Z, Dong Y, Scholz R, Neumann D, Zou MH. Phosphorylation of LKB1 at serine 428 by protein kinase C-zeta is required for metformin-enhanced activation of the AMP-activated protein kinase in endothelial cells. Circulation 2008;117:952–962

24. Li H, Lee J, He C, Zou MH, Xie Z. Suppression of the mTORC1/STAT3/Notch1 pathway by activated AMPK prevents hepatic insulin resistance induced by excess amino acids. Am J Physiol Endocrinol Metab 2014;306:E197–E209

25. Li H, Min Q, Ouyang C, et al. AMPK activation prevents excess nutrient-induced hepatic lipid accumulation by inhibiting mTORC1 signaling and

endoplasmic reticulum stress response. Biochim Biophys Acta 2014;1842:1844–1854

26. He C, Zhu H, Zhang W, et al. 7-Ketocholesterol induces autophagy in vascular smooth muscle cells through Nox4 and Atg4B. Am J Pathol 2013;183:626–637

27. Wang S, Zhang M, Liang B, et al. AMPKalpha2 deletion causes aberrant expression and activation of NAD(P)H oxidase and consequent endothelial dysfunction in vivo: role of 26S proteasomes. Circ Res 2010;106:1117–1128

28. He C, Choi HC, Xie Z. Enhanced tyrosine nitration of prostacyclin synthase is associated with increased inflammation in atherosclerotic carotid arteries from type 2 diabetic patients. Am J Pathol 2010;176:2542–2549

29. Ruderman N, Prentki M. AMP kinase and malonyl-CoA: targets for therapy of the metabolic syndrome. Nat Rev Drug Discov 2004;3:340–351

30. Darnell JE Jr, Kerr IM, Stark GR. Jak-STAT pathways and transcriptional activation in response to IFNs and other extracellular signaling proteins. Science 1994;264:1415–1421

31. Marrero MB, Schieffer B, Paxton WG, et al. Direct stimulation of Jak/STAT pathway by the angiotensin II AT1 receptor. Nature 1995;375:247–250

32. Liu D, Scafidi J, Prada AE, Zahedi K, Davis AE 3rd. Nuclear phosphatases and the proteasome in suppression of STAT1 activity in hepatocytes. Biochem Biophys Res Commun 2002;299:574–580

33. Venema RC, Venema VJ, Eaton DC, Marrero MB. Angiotensin II-induced tyrosine phosphorylation of signal transducers and activators of transcription 1 is regulated by Janus-activated kinase 2 and Fyn kinases and mitogen-activated protein kinase phosphatase 1. J Biol Chem 1998;273:30795–30800

34. Ichikawa T, Zhang J, Chen K, et al. Nitroalkenes suppress lipopolysaccharide-induced signal transducer and activator of transcription signaling in macrophages: a critical role of mitogen-activated protein kinase phosphatase 1. Endocrinology 2008;149:4086–4094

35. Brondello JM, Pouysségur J, McKenzie FR. Reduced MAP kinase phosphatase-1 degradation after p42/p44MAPK-dependent phosphorylation. Science 1999;286:2514–2517

36. Viana R, Aguado C, Esteban I, et al. Role of AMP-activated protein kinase in autophagy and proteasome function. Biochem Biophys Res Commun 2008;369:964–968

37. Frank DA, Mahajan S, Ritz J. Fludarabine-induced immunosuppression is associated with inhibition of STAT1 signaling. Nat Med 1999;5:444–447

38. Torella D, Curcio A, Gasparri C, et al. Fludarabine prevents smooth muscle proliferation in vitro and neointimal hyperplasia in vivo through specific inhibition of STAT-1 activation. Am J Physiol Heart Circ Physiol 2007;292:H2935–H2943

39. Dong Y, Zhang M, Liang B, et al. Reduction of AMP-activated protein kinase alpha2 increases endoplasmic reticulum stress and atherosclerosis in vivo. Circulation 2010;121:792–803

40. Zhao Q, Ishibashi M, Hiasa K, Tan C, Takeshita A, Egashira K. Essential role of vascular endothelial growth factor in angiotensin II-induced vascular inflammation and remodeling. Hypertension 2004;44:264–270

41. Savoia C, Schiffrin EL. Vascular inflammation in hypertension and diabetes: molecular mechanisms and therapeutic interventions. Clin Sci (Lond) 2007;112:375–384

42. Oka T, Hikoso S, Yamaguchi O, et al. Mitochondrial DNA that escapes from autophagy causes inflammation and heart failure. Nature 2012;485:251–255

43. Chang MY, Ho FM, Wang JS, et al. AICAR induces cyclooxygenase-2 expression through AMP-activated protein kinase-transforming growth factor-beta-activated kinase 1-p38 mitogen-activated protein kinase signaling pathway. Biochem Pharmacol 2010;80:1210–1220

44. Meares GP, Qin H, Liu Y, Holdbrooks AT, Benveniste EN. AMP-activated protein kinase restricts IFN-γ signaling. J Immunol 2013;190:372–380

45. Vasamsetti SB, Karnewar S, Kanugula AK, Raj AT, Kumar JM, Kotamraju S. Metformin inhibits monocyte-to-macrophage differentiation via AMPK mediated inhibition of STAT3 activation: Potential role in atherosclerosis. Diabetes 31 December 2014 [Epub ahead of print]. DOI: 10.2337/db14-1225

46. Nerstedt A, Johansson A, Andersson CX, Cansby E, Smith U, Mahlapuu M. AMP-activated protein kinase inhibits IL-6-stimulated inflammatory response in human liver cells by suppressing phosphorylation of signal transducer and activator of transcription 3 (STAT3). Diabetologia 2010;53: 2406–2416

47. Slack DN, Seternes OM, Gabrielsen M, Keyse SM. Distinct binding determinants for ERK2/p38alpha and JNK map kinases mediate catalytic activation and substrate selectivity of map kinase phosphatase-1. J Biol Chem 2001;276: 16491–16500

48. Wang X, Zhao Q, Matta R, et al. Inducible nitric-oxide synthase expression is regulated by mitogen-activated protein kinase phosphatase-1. J Biol Chem 2009; 284:27123–27134

49. Aghdam SY, Gurel Z, Ghaffarieh A, Sorenson CM, Sheibani N. High glucose and diabetes modulate cellular proteasome function: Implications in the pathogenesis of diabetes complications. Biochem Biophys Res Commun 2013;432:339–344

50. Weng Y, Shen F, Li J, Shen Y, Zhang X. Expression changes of mitogen-activated protein kinase phosphatase-1 (MKP-1) in myocardium of streptozotocin-induced diabetic rats. Exp Clin Endocrinol Diabetes 2007;115:455–460